

Low-noise submicron channel graphene nanoribbons

Guangyu Xu,^{1,a)} Jingwei Bai,² Carlos M. Torres, Jr.,¹ Emil B. Song,¹ Jianshi Tang,¹ Yi Zhou,¹ Xiangfeng Duan,³ Yuegang Zhang,⁴ and Kang L. Wang¹

¹Department of Electrical Engineering, University of California at Los Angeles, Los Angeles, California 90095, USA

²Department of Material Science and Engineering, University of California at Los Angeles, Los Angeles, California 90095, USA

³Department of Chemistry and Biochemistry, University of California at Los Angeles, Los Angeles, California 90095, USA

⁴Molecular Foundry, Lawrence Berkeley National Laboratory, Berkeley, California 94720, USA

(Received 2 June 2010; accepted 30 July 2010; published online 18 August 2010)

We present a graphene nanoribbon fabrication method based on a nanowire mask. Using a four-probe setup, single-layer nanoribbon (SLR) and bilayer nanoribbon (BLR) show low-frequency noise levels lower than (comparable to) the SLRs (BLRs) achieved by hydrogen-silsesquioxane based methods. Submicron channel SLR and BLR both show conductance quantization at 77 K, which suggests that quasi-one-dimensional quantum transport can be achieved. The conductance plateaus in BLR are less pronounced than those in SLR. © 2010 American Institute of Physics. [doi:10.1063/1.3481351]

Graphene nanoribbon (GNR) is a quasi-one-dimensional (quasi-1D) film, in which a band gap exists through either the quantum confinement, localization effect or the spatial charge inhomogeneity.^{1–6} Compared to the bulk graphene with a micron-sized width, GNR has great potential in achieving high $I_{\text{on}}/I_{\text{off}}$ ratio.^{2,4,6} Most reported GNRs, however, are degraded by compositional disorders.^{7–9} For example, GNRs patterned using electron beam lithography processes is limited by the spot size of the electron beam and the doping effects from residuals of hydrogen-silsesquioxane (HSQ).^{2,7} Moreover, the trapping/detrapping processes occurring near GNR significantly affect the device stability;¹⁰ the resulting conductance fluctuations contribute to the low-frequency noise, which lowers the signal-to-noise ratio and increases the phase distortion in rf applications.¹¹ Hence, rational GNR patterning methods are needed to achieve high-quality devices with low-noise level, which is critical to realize GNR applications with low power consumption and energy delay products.

In this work, we present the low-noise GNRs achieved by a nanowire-mask based fabrication method. This method improves the GNR surface cleanliness by avoiding HSQ resist residual, and eases the fabrication by using only one-step e-beam lithography.² Using a four-probe setup, single layer nanoribbon (SLR) and bilayer nanoribbon (BLR) devices show low-frequency noise levels lower than (comparable to) the SLRs (BLRs) achieved by HSQ based methods.¹¹ Quasi-1D quantum transport can be realized in both submicron channel SLR and BLR at 77 K;^{7,12} this fact reaffirms the high-quality of the GNRs.

Bulk graphene sheets are mechanically exfoliated from natural graphite and transferred onto a 300 nm thermally grown SiO₂ dielectric film on highly doped Si substrates, and confirmed by Raman spectroscopy.¹ Then, silicon nanowires are deposited onto the graphene sheets to serve as an etch mask (diameter ranging from 20 to 50 nm) and located by means of an optical microscope¹³ [see Fig. 1(a)]. A 30 s low

power oxygen plasma process is applied to etch away the exposed graphene, leaving the GNR beneath the nanowires untouched.¹³ The nanowires are then removed by weak sonication in deionized water followed by isopropyl alcohol rinsing, in order to leave only the GNRs on the SiO₂ substrate. Finally, the GNRs are patterned into multiprobe structures by e-beam lithography with Ti/Au electrodes (7 nm/80 nm) [see Fig. 1(b)]. All GNRs are scanned by atomic force microscopy (AFM) for dimension inspection¹⁴ [see Fig. 1(c)]. The devices were maintained in vacuum environment to avoid

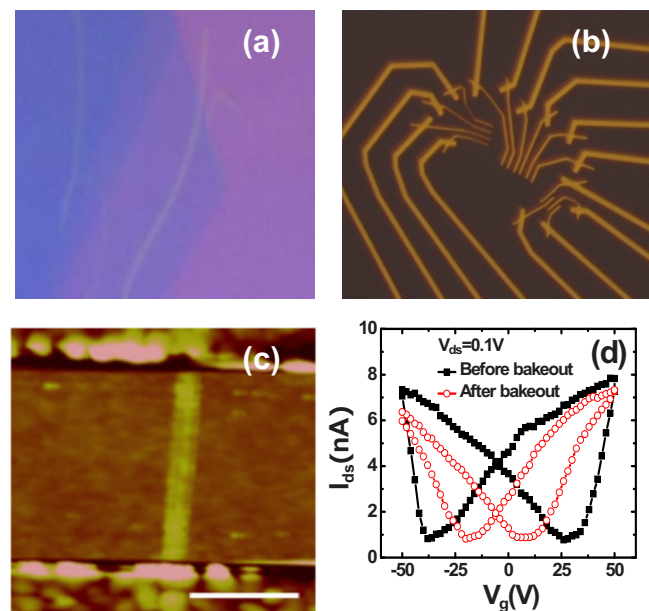


FIG. 1. (Color online) Nanowire-mask based methods for GNR device fabrication. (a) Nanowire patterned onto single layer (middle) and multilayer (left) bulk graphene sheet on top of 300 nm SiO₂ layer (right). (b) Fabricated SLR devices. Three nanoribbons were defined by the nanowire patterning. The distance of the nearest two Ti/Au electrodes is generally less than 500 nm. (c) AFM image of SLR (L ~ 875 nm, W ~ 70 nm) after fabrication. The scale bar equals 0.3 μm . (d) Effect of vacuum bakeout processes on the $I_{\text{ds}}-V_g$ curves. A dual-sweep of gate biases was applied to illustrate the hysteresis effect before and after the bake out process.

^{a)}Electronic mail: guangyu@ee.ucla.edu.

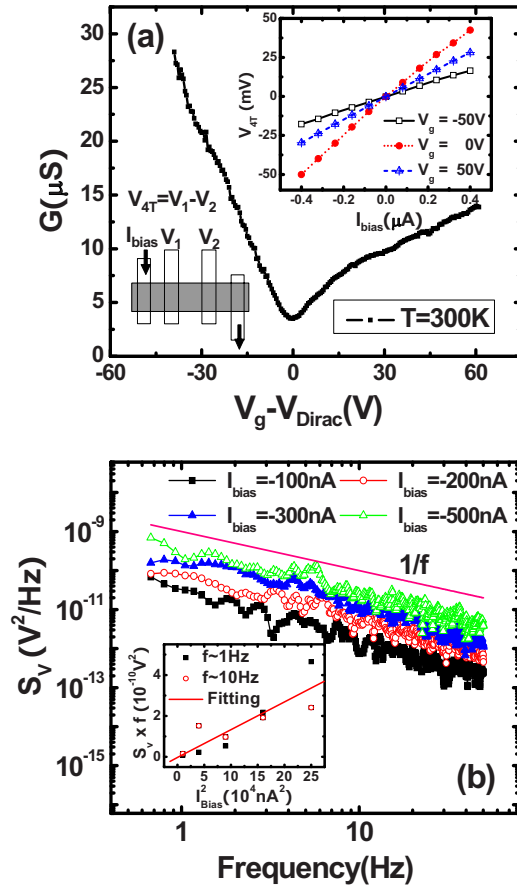


FIG. 2. (Color online) Four-probe conductance and low-frequency noise measurements of SLR at $T=300$ K. (a) G - V_g curve in a four-terminal setup (left inset). The device was biased in the linear regime (right inset) at all gate biases. (b) Low-frequency noise spectra of a SLR ($L \sim 405$ nm, $W \sim 36$ nm) away from the Dirac point ($V_g - V_{\text{Dirac}} = 40$ V). The noise spectra follow $1/f^\alpha$ behavior with α ranging from 0.85 to 1.12. The solid line shows the normalized $1/f$ noise scaled to $S_V = 9.55 \times 10^{-10}$ V²/Hz at $f \sim 1$ Hz. The inset shows that the frequency normalized noise at both $f \sim 1$ Hz and $f \sim 10$ Hz is proportional to I_{bias}^2 .

contact oxidation and doping effects from the ambience. A 20 min vacuum bakeout (100 °C) process is applied to desorb contaminants before the transport and noise measurement.¹⁵ The vacuum baking process remarkably improves the device hysteresis (typically < 20 V) [see Fig. 1(d)]. The yield exceeds 90% out of more than 70 fabricated GNRs.

Till now, most GNRs with two-probe structures were used to investigate the transport within the band gap, where a bulk graphene was connected to GNR to reduce the metal-contact resistance and the GNR (rather than the bulk graphene) determined the gap feature.^{1-7,12} This structure, however, can obscure the intrinsic transport and noise characteristics of GNRs outside the band gap where the bulk graphene might contribute the serial resistance and extra noise.¹⁶ Here we use a standard four-probe device structure for dc transport and noise measurement, in order to eliminate the effects of serial bulk graphene in a two-probe structure. An Agilent 4156C was used to apply dc current bias to the device in its linear regime [see the upper inset of Fig. 2(a)], and its dc conductance (G) was measured; an Agilent 35670A was used to collect the noise spectra of the fluctuations of the potential difference (V) across the GNRs [see the lower inset of Fig. 2(a)]. At a certain gate bias (V_g), the

conductance is averaged by ten times of measurements at the same time of the noise measurement to avoid the hysteresis and ensure the consistency of the data.¹⁶

GNRs are current-biased in the linear regime [$> 90\%$ linearity from the low-bias I_{bias} - V_{4T} curves: I_{bias} and V_{4T} are the current bias and the potential drop across the GNR, see the insets of Fig. 2(a)] for measuring G at each V_g .⁶ Figure 2(a) shows the G - V_g curve of a typical SLR at 300 K (shifted by the gate bias at the Dirac point, V_{Dirac}). The electron-hole asymmetry in our four-probe measurement may result from the extrinsic doping effect of the Ti/Au metal contacts, which forms the local p-n or p-p junction near the metal/GNR interface depending on the types of carriers.¹⁷⁻¹⁹ Correspondingly, Fig. 2(b) shows the typical low-frequency noise spectra, S_V , (after subtracting the background noise, which was measured at zero current bias) at $V_g - V_{\text{Dirac}} = 40$ V, with I_{Bias} varying from -100 to -500 nA. The noise follows the $1/f^\alpha$ behavior (α ranges from 0.85 to 1.12) for the frequency (f) range from 0.05 to 50 Hz. Some deviation of the $1/f$ shape may be induced by few large random telegraph signals from individual traps, which have a Lorentzian noise characteristic of their own.¹⁶ We further normalized the noise level by frequency as $S_V \times f$. The normalized noise data from $f \sim 1$ Hz and $f \sim 10$ Hz are both proportional to I_{bias} (Ref. 2) [see the inset of Fig. 2(b)], which follows the Hooge's law $S_V \sim V^2$ (see Ref. 20). This fact confirms that the noise is from trap-induced conductance fluctuations, and the current-induced local heating effect is not significant here.^{10,21}

To quantify the noise level, Lin and Avouris defined the normalized noise figure $\eta = (A/R) \times L^2$ in Ref. 11: the noise figure A was given as $A = S_1 \cdot f / I^2$ in two-probe setup (S_1 is the noise spectra of current fluctuations); R and L are the resistance and channel-length of GNRs, respectively. This definition could be used to compare the noise level for GNRs with different dimensions. To reduce the measurement error at certain frequencies, we define the frequency averaged noise figure $A = (1/N) \sum_{i=1}^N f_i \cdot S_{V_i} / V^2$ in four-probe setup, where N is the number of frequencies. Away from V_{Dirac} ($V_g - V_{\text{Dirac}} = 40$ V), we estimate that our SLR (with the measured width/length, $W/L \sim 36$ nm/406 nm) features a noise as low as $\eta_{\text{SLR}} \sim 6.4 \times 10^{-12}$ $\mu\text{m}^2/\Omega$ for the resistance per unit length ($R/L \sim 80$ k $\Omega/\mu\text{m}$ which is lower than those ($\eta_{\text{SLR}} \sim \text{constant} \sim 1.0 \times 10^{-11}$ $\mu\text{m}^2/\Omega$) achieved by HSQ-based methods.¹¹ The low noise of SLRs using our nanowire-based method can relate to the following reasons: (1) The SLR is not covered/contaminated by HSQ residues, which act as extra traps and contribute to the noise; (2) the noise in two-probe device can result from the conductance fluctuations induced by traps both in the channel and near the contacts.^{16,22} Thus, our four-probe setup reduces the noise originating from the traps near the contacts and the connected bulk graphene as the case in two-probe setup.¹¹ AFM inspection shows a nonuniformity of the width less than 10 nm in our SLRs, comparable to those achieved in HSQ-based methods. Surface engineering of the Si nanowire may further improve this.

Similarly, $1/f$ noise spectra for our BLR ($W/L = 60$ nm/712 nm) are also collected at $V_g - V_{\text{Dirac}} = 40$ V (not shown). The noise level $\eta_{\text{BLR}} \sim 1.05 \times 10^{-12}$ $\mu\text{m}^2/\Omega$ for $R/L \sim 376$ k $\Omega/\mu\text{m}$ is comparable to those achieved by HSQ-based BLRs. Consistent with Lin *et al.*,¹¹ we observe overall a lower noise level in BLR than SLR with similar

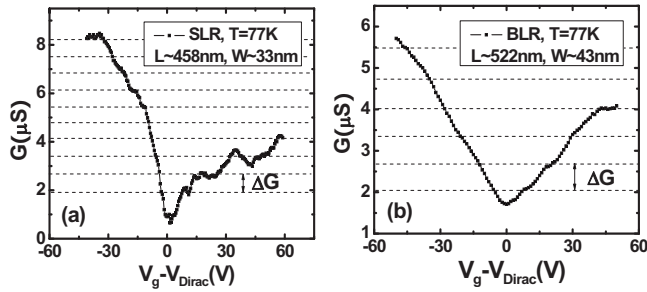


FIG. 3. Four-probe transport properties of SLR and BLR at $T=77$ K. (a) G - V_g curves of a SLR ($L\sim 458$ nm, $W\sim 33$ nm). (b) G - V_g curves of a BLR ($L\sim 522$ nm, $W\sim 43$ nm). The conductance quantization was observed at 77 K for both SLR and BLR. Horizontal dashed lines are guides for eyes, showing the quantization spacing of the conductance $\Delta G_{\text{SLR}}\sim 0.7$ μS and $\Delta G_{\text{BLR}}\sim 0.6$ μS , respectively.

channel dimensions, which may result from more effective screening to traps in BLR.¹¹ So far, the work on BLR transport is rare.^{23,24} The reason that our BLR does not show as much noise reduction (comparing to HSQ-based BLRs) as SLR is not clear to us for now.

Finally, we observed the quantized conductance at $T=77$ K for both SLR and BLR, which suggests that quasi-1D quantum transport can be achieved by this method.^{7,12} Figures 3(a) and 3(b) show the G - V_g curves of SLR and BLR, respectively, where the quantized conductance spacing, ΔG , are nearly constant.²⁵ Some features are discussed as follows: (1) the main conductance plateaus remain when we change the gate sweeping directions (not shown), ruling out the mobile-ion-induced hysteresis effect;¹⁶ (2) the conductance plateaus is defined by the density-of-state of quasi-1D transport system.⁷⁻⁹ Some deviation may come from compositional types of disorders existing in GNRs such as the edge states, bulk vacancies and the charged impurities near the GNR.^{9,26-28} Contact-induced doping can also destroy the quasi-1D transport of GNRs; (3) the conductance plateaus in BLR are less pronounced than those in SLR. This can be understood as the smaller energy separation of subbands in BLR defined as its subband structures;²³ thus the conductance plateaus can be smeared by the temperature and disorder more easily. We repeated the measurements for more than 30 devices to confirm that the quantized conductance is observable with L up to 1.1 μm for both SLR and BLR.

In summary, this work presents a fabrication method of high-quality GNR devices based on a nanowire mask. Four-probe $1/f$ noise spectra were collected to examine the sensitivity of the GNRs to the interface traps. The noise level of SLR is lower than that achieved by HSQ-mask based methods, possibly because our samples are free of both HSQ coverage/residual and noise contribution from the contacts as in two-probe setups. The observed conductance quantization in submicron channel SLR and BLR suggests that the quasi-1D transport is achievable at $T=77$ K. The conductance plateaus in BLR are less pronounced than those in SLR

possibly due to its subband structure. This GNR fabrication method may help improve the signal-to-noise-ratio of GNR devices and promote applications of quantum transport in graphene materials.

This work was in part supported by MARCO Focus Center on Functional Engineered Nano Architectonics (FENA). The work at the Molecular Foundry was supported by the U.S. Department of Energy under Contract No. DE-AC02-05CH11231.

- ¹M. Y. Han, B. Ozyilmaz, Y. Zhang, and P. Kim, *Phys. Rev. Lett.* **98**, 206805 (2007).
- ²Z. Chen, Y. M. Lin, M. J. Rooks, and P. Avouris, *Physica E (Amsterdam)* **40**, 228 (2007).
- ³F. Sols, F. Guinea, and A. H. Castro Neto, *Phys. Rev. Lett.* **99**, 166803 (2007).
- ⁴C. Stampfer, J. Guettinger, S. Hellmueller, F. Molitor, K. Ensslin, and T. Ihn, *Phys. Rev. Lett.* **102**, 056403 (2009).
- ⁵P. Gallagher, K. Todd, and D. Goldhaber-Gordon, *Phys. Rev. B* **81**, 115409 (2010).
- ⁶M. Y. Han, J. C. Brant, and P. Kim, *Phys. Rev. Lett.* **104**, 056801 (2010).
- ⁷Y. M. Lin, V. Perebeinos, Z. Chen, and P. Avouris, *Phys. Rev. B* **78**, 161409(R) (2008).
- ⁸E. R. Mucciolo, A. H. Castro Neto, and C. H. Lewenkopf, *Phys. Rev. B* **79**, 075407 (2009).
- ⁹S. Ihnatsenka and G. Kirczenow, *Phys. Rev. B* **80**, 201407(R) (2009).
- ¹⁰A. van der Ziel, *Proc. IEEE* **76**, 233 (1988).
- ¹¹Y. M. Lin and P. Avouris, *Nano Lett.* **8**, 2119 (2008).
- ¹²C. Lian, K. Tahy, T. Fang, G. Li, H. G. Xing, and D. Jena, *Appl. Phys. Lett.* **96**, 103109 (2010).
- ¹³J. Bai, X. Duan, and Y. Huang, *Nano Lett.* **9**, 2083 (2009).
- ¹⁴X. Wang, Y. Ouyang, X. Li, H. Wang, J. Guo, and H. Dai, *Phys. Rev. Lett.* **100**, 206803 (2008).
- ¹⁵J.-H. Chen, C. Jang, S. Adam, M. S. Fuhrer, E. D. Williams, and M. Ishigami, *Nat. Phys.* **4**, 377 (2008).
- ¹⁶G. Xu, F. Liu, S. Han, K. Ryu, A. Badmaev, B. Lei, C. Zhou, and K. L. Wang, *Appl. Phys. Lett.* **92**, 223114 (2008).
- ¹⁷E. J. H. Lee, K. Balasubramanian, R. T. Weitz, M. Burghard, and K. Kern, *Nat. Nanotechnol.* **3**, 486 (2008).
- ¹⁸B. Huard, N. Stander, J. A. Sulpizio, and D. Goldhaber-Gordon, *Phys. Rev. B* **78**, 121402(R) (2008).
- ¹⁹G. Giovannetti, P. A. Khomyakov, G. Brocks, V. M. Karpan, J. van den Brink, and P. J. Kelly, *Phys. Rev. Lett.* **101**, 026803 (2008).
- ²⁰F. N. Hooge, *IEEE Trans. Electron Devices* **41**, 1926 (1994).
- ²¹Y.-W. Tan, Y. Zhang, K. Bolotin, Y. Zhao, S. Adam, E. H. Hwang, S. Das Sarma, H. L. Stormer, and P. Kim, *Phys. Rev. Lett.* **99**, 246803 (2007).
- ²²D. Tobias, M. Ishigami, A. Tselev, P. Barbara, E. D. Williams, C. J. Lobb, and M. S. Fuhrer, *Phys. Rev. B* **77**, 033407 (2008).
- ²³H. Xu and T. Heinzel, *Phys. Rev. B* **80**, 045308 (2009).
- ²⁴X. Li, Z. Zhang, and D. Xiao, *Phys. Rev. B* **81**, 195402 (2010).
- ²⁵For BLR, the quantization spacing ΔG near the transition of main conductance plateaus are nearly constant. No other detail conductance plateaus are observed at $T=77$ K as predicted in disordered BLRs (Ref. 23), possibly because they are smeared by the temperature.
- ²⁶H. Şahin and R. T. Senger, *Phys. Rev. B* **78**, 205423 (2008).
- ²⁷The bulk vacancies are atomic defects away from the GNR edges, which suppress the conductance level and smear the conductance plateaus from the ideal quasi-1D case (Ref. 9). In our GNRs, their impact should be small as indicated by a small D-peak intensity in Raman spectroscopy (not shown) (Ref. 14).
- ²⁸D. Gunlycke, J. Li, J. W. Mintmire, and C. T. White, *Appl. Phys. Lett.* **91**, 112108 (2007).